

## Research Article

# Comparison of Satellite and Ground-Based Phenology in China's Temperate Monsoon Area

Huanjiong Wang,<sup>1,2</sup> Junhu Dai,<sup>1</sup> and Quansheng Ge<sup>1</sup>

<sup>1</sup> Institute of Geographical Sciences and Natural Resources Research, Chinese Academy of Sciences, A 11 Datun Road, Chaoyang District, Beijing 100101, China

<sup>2</sup> University of Chinese Academy of Sciences, 19A Yuquan Road, Beijing 100049, China

Correspondence should be addressed to Junhu Dai; [daijh@igsrr.ac.cn](mailto:daijh@igsrr.ac.cn) and Quansheng Ge; [geqs@igsrr.ac.cn](mailto:geqs@igsrr.ac.cn)

Received 12 February 2014; Revised 20 March 2014; Accepted 20 March 2014; Published 24 April 2014

Academic Editor: Dong Jiang

Copyright © 2014 Huanjiong Wang et al. This is an open access article distributed under the Creative Commons Attribution License, which permits unrestricted use, distribution, and reproduction in any medium, provided the original work is properly cited.

Continuous satellite datasets are widely used in tracking vegetation responses to climate variability. Start of season (SOS), for example, can be derived using a number of methods from the time series of satellite reflectance data; however, various methods often produce different SOS measures which limit the application of satellite data in phenological studies. Therefore, we employed five methods to estimate SOS from the Advanced Very High Resolution Radiometer (AVHRR)/normalized difference vegetation index (NDVI) dataset. Subsequently, we compared the SOS with the ground-based first leaf date (FLD) of 12 deciduous broadleaved plant species at 12 sites of the Chinese Phenological Observation Network (CPON). The results show that the latitudinal patterns of five satellite-derived SOS measures are similar to each other but different from the pattern of ground phenology. For individual methods, the variability of SOS time series is significantly different from ground phenology except for HANTS, Polyfit, and Midpoint methods. The SOS calculated using the Midpoint method showed significant correlations with ground phenophases most frequently (in 47.1% of cases). Using the SOS derived from the Midpoint method, significantly earlier trends in SOS were detected in 50.7% of the natural vegetation area from 1982 to 2006.

## 1. Introduction

Phenology, as the study of periodic biological events in the animal and plant world [1], occupies an important position in global change science. Long-term phenological data can provide independent evidence for the effects of environmental change [2, 3]. Impacted by recent climate change [4, 5], trends toward earlier plant phenophases in spring have been observed in many places around the world [6, 7].

Such phenological shifts can influence many properties of terrestrial ecosystems [4, 9]. It is reported that plant phenology is tightly coupled with the seasonal cycles of surface carbon and energy balances in boreal forest ecosystems in western Canada [10]. Modeled spring indices (SI), first bloom date, could serve as proxy for both average spring net ecosystem exchange (NEE) drawdown date and latent-sensible heat crossover date in deciduous forests [11]. Earlier spring onset in combination with delays in the end of the

growing season has also resulted in enhanced vegetation growth in the Northern Hemisphere over the past two decades [12].

Before recent technological advances, the most conventional means to monitor phenological dynamic in plants was through manually recorded human observations at discrete intervals. Recently, researchers began to use eddy covariance towers and satellite sensors to assist in monitoring phenological change on larger spatial scales [4]. Remote sensing phenology or land surface phenology (LSP), defined as the seasonal pattern of variation in vegetated land surfaces observed from remote sensing [13], is the focus of this study. We chose a primary phenological marker—the start of season (SOS)—as the object of this study. The SOS is also called the green-up date, the onset of greenness, or the start of the growing season.

The multiple SOS method can lead to distinct estimates in the same region [14, 15]. For example, based on different

methods, the trends of advance in SOS for China's temperate region ranged from 2.25 days decade<sup>-1</sup> [16] to 7.9 days decade<sup>-1</sup> [17]. Therefore, the accuracy of SOS methods needs to be carefully evaluated according to ground phenology data. To address this problem, White et al. [18] performed a comprehensive intercomparison of ten SOS methods over broad regions of North America based on ground phenology data and cryospheric/hydrologic seasonality metrics. Schwartz and Hanes [11] further added the latent-sensible heat flux and carbon flux data into the comparison. A comparative study of satellite and ground-based phenology was also made in Switzerland [19]. These studies suggested that not all methods were closely related to ground observations. In temperate China, the accuracy of multiple SOS methods has not been assessed.

As the Institute of Geographical Sciences and Natural Resources Research (IGSNRR) at the Chinese Academy of Sciences has administered the Chinese Phenological Observation Network (CPON) and accumulated a solid database in recent years, we can thoroughly compare Phenological trends derived from remote sensing with those of ground observations and assess the accuracy of different SOS methods. In this study, we employed five methods to estimate SOS for China's temperate monsoon area using a consistently processed satellite dataset. Subsequently, we analyzed the relationships between different SOS measures and ground first leaf dates (FLD) at 12 CPON sites, evaluating which estimation methods for SOS were the best. As a result, we estimated 1982–2006 trends in SOS based on those methods that were most consistent with ground data.

## 2. Materials and Methods

**2.1. Study Area.** The temperate monsoon area, located in north and northeast China, was chosen as the study area (Figure 1). Mean annual temperature in this area ranges from  $-4$  to  $14^{\circ}\text{C}$ , while mean annual precipitation decreases from 800 mm in the southeast to 400 mm in the northwest. Affected by the East Asian monsoon, precipitation mainly falls between June and August. The primary natural vegetation in this area, as identified from a digitized 1:1,000,000 vegetation map of China [20], includes needleleaf forests, needleleaf and broadleaf mixed forests, and broadleaf forests.

**2.2. Ground and Satellite Dataset.** Ground phenological data are derived from CPON, which began its observations in 1963 under the auspices of IGSNRR at the Chinese Academy of Sciences. In this study, data collected from 1982 to 2006 on twelve species of deciduous broadleaved trees and one phase (first leaf date (FLD)) at 12 CPON sites were compared (Figure 1 and Table 1). According to the uniform observation criteria and guidelines of CPON [21], the FLD is defined as the date when a plant forms its first fully unfolded leaf. A total of 85 different cases were therefore available, with one case consisting of a phenological time series at a specific site (Table 1). The FLD time series are not continuous because no observations were carried out in certain periods at each site. Because the missing observation data affects the analysis, the

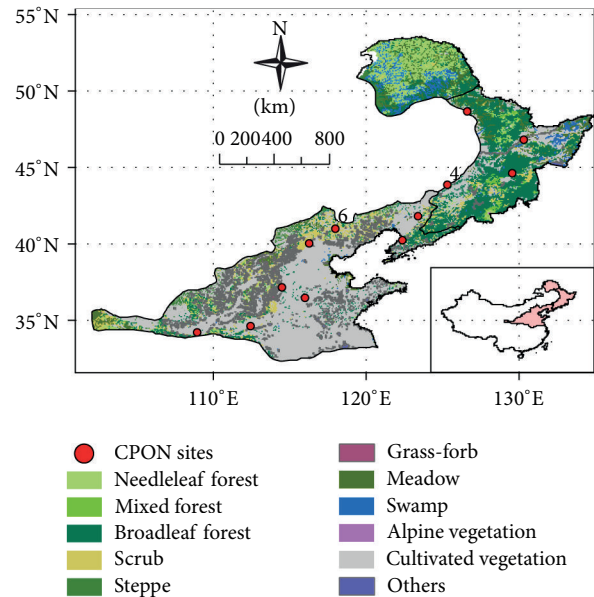


FIGURE 1: Distribution of vegetation types in China's temperate monsoon area and the twelve sites from Chinese Phenological Observation network (CPON) in this study.

missing data are estimated using a phenological model that is driven by temperature data from a nearby weather station. This gap-filling method was described in Ge et al. [8].

With respect to the satellite data, we obtained the data set produced by the Global Inventory Monitoring and Modeling Studies (GIMMS) group of the normalized difference vegetation index (NDVI) for the period 1982 to 2006 at a spatial resolution of 8 km and 15 day intervals. This dataset was observed by Advanced Very High Resolution Radiometer (AVHRR) instruments aboard the NOAA satellite series 7, 9, 11, 14, 16, and 17 and has been corrected for calibration, view geometry, volcanic aerosols, and other effects not related to vegetation change [22]. Sparsely vegetated pixels with annual mean NDVI of less than 0.1 have been excluded to reduce the impact of bare soils [23]. In addition, pixels with cultivated vegetation [20] are excluded because the phenology of cultivated vegetation is strongly impacted by human activity.

**2.3. Estimation of SOS.** There are several methods to extract SOS from the NDVI dataset. These methods usually consist of two steps [15]. The first step was to reconstruct continuous and daily NDVI series with the noise removed by using curve approaches, such as a polynomial function [17], piecewise logistic functions [24], a Fourier filter [25], spline functions [26, 27], or a Savitzky-Golay filter [28, 29]. In the next step, critical thresholds for SOS were determined from the reconstructed NDVI time series.

Five approaches are commonly used to determine SOS thresholds: (1) thresholds defined by the timing of the greatest relative change in multiyear averaged NDVI series, where

TABLE 1: Study species and their distribution sites with first leaf date (FLD) data. The number of sites for each species is defined in Figure 1.

No.	Species	Phase	Distribution sites	Number of sites
1	<i>Ailanthus altissima</i>	FLD	5, 7, 8, 9, 11, 12	6
2	<i>Salix babylonica</i>	FLD	3, 5, 7, 9, 10, 11, 12	7
3	<i>Robinia pseudoacacia</i>	FLD	5, 6, 7, 8, 9, 10, 11, 12	8
4	<i>Salix matsudana</i>	FLD	1, 3, 5, 7, 8, 9, 10	7
5	<i>Sophora japonica</i>	FLD	6, 9, 10, 11, 12	5
6	<i>Populus × canadensis</i>	FLD	1, 5, 6, 8, 9, 10, 11, 12	8
7	<i>Morus alba</i>	FLD	7, 8, 9, 12	4
8	<i>Amygdalus davidiana</i>	FLD	4, 5, 6, 8, 12	5
9	<i>Armeniaca vulgaris</i>	FLD	2, 3, 7, 8, 9, 10, 12	7
10	<i>Ulmus pumila</i>	FLD	1, 2, 3, 4, 5, 7, 8, 9, 10, 11, 12	11
11	<i>Amygdalus triloba</i>	FLD	1, 2, 4, 7, 8, 9, 12	7
12	<i>Syringa oblata</i>	FLD	1, 2, 4, 5, 6, 7, 8, 9, 11, 12	10

the corresponding NDVI ( $t$ ) is determined as the NDVI threshold for SOS, where  $t$  is the time with the maximum relative NDVI increase [17]; it is worth noting that the SOS threshold is constant for each pixel and does not change with time; (2) maximum relative change, where the SOS is determined as the date with the maximum relative change of NDVI [30]; (3) maximum increase, where the NDVI time series is firstly transformed to its first derivate; in each year, maximum of first derivate marks the SOS [19]; (4) Midpoint, whereby the NDVI time series is first transformed to 0-1 NDVI<sub>ratio</sub>; Then the SOS is defined as the day of the year when 0.5 NDVI<sub>radio</sub> is exceeded [26]; and (5) 20% of NDVI amplitude, where the SOS is defined as the date when the NDVI has increased 20% of the seasonal amplitude from the growing season minimum level [31]. These five methods (Polyfit, Logistic, HANTS, Midpoint, and Timesat) are summarized in Table 2. Specially, in the Logistic method, Zhang et al. [24] recognized that the SOS corresponds to the times at which the rate of change in curvature in the vegetation index data exhibits first local maximums. Other studies have, however, suggested that this metric may be sensitive to early spring understory growth [32], so we utilize the approach of maximum relative change instead (Table 2). All of these five methods were used to estimate SOS for each pixel in the study area over the 1982–2006 period.

**2.4. Comparisons and Analyses.** We firstly calculated the mean FLD from 1982 to 2006 for each CPON site as well as the mean of satellite-derived SOS measures for each pixel. Then we compared the latitudinal patterns of ground phenophases and five satellite-derived SOS measures. Second, we calculated the coefficient of variation (CV) for ground FLD time series at each site and five satellite-derived SOS measures in pixels with broadleaf forest from 1982 to 2006. Through one-way analysis of variance (ANOVA) and Tukey multiple comparison [34], we assessed the variability of satellite-derived SOS measures. Third, at each site, we calculated Pearson's correlation coefficients between the FLD time series of each tree species as well as SOS time series averaged from

the closest 49 pixels (excepting cultivated vegetation). Last, we selected the SOS method, the most consistent with the ground phenology, and performed the regression analysis between SOS time series and year for each pixel. The SOS trend is represented by the slope of the regression model.

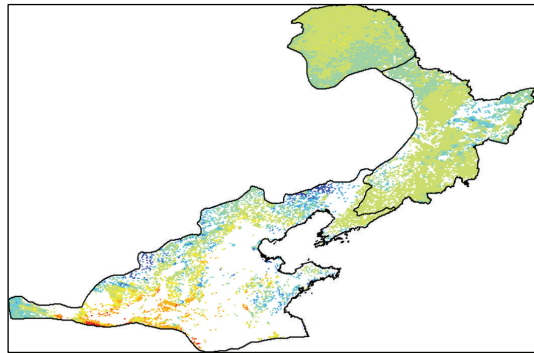
### 3. Results

**3.1. Assessment of Spatial Patterns for Variations of SOS.** At first, we studied the spatial pattern of SOS averaged over five SOS measures in the 1982 to 2006 period. The south to north progression of spring phenological events in the study area is shown to be delayed. Mean SOS is delayed from the south to the central study region and then becomes slightly earlier in the northeast region (Figure 2(a)). The SOS in the Changbai Mountains (N38°46'–47°30', E121°08'–134°) is later than the surrounding area. With regard to the vegetation types, the SOS of the steppe occurs on 16 May, which is the latest. Grass-forb, meadow, swamp, and alpine vegetation have similar SOS patterns ranging from 2 May to 4 May. SOS of needleleaf forest, mixed forest, broadleaf forest, and scrub is the earliest (April 27–30). Individual methods often differ in SOS measures, especially in North China. Across the study area, the maximum differences among the five satellite-derived SOS measures range from 19 to 100 days with a mean of 43 days (Figure 2(b)), suggesting that different SOS methods may detect different portions of the annual vegetation development cycle.

For broadleaf forest, the latitudinal patterns of SOS derived from the five satellite measures are consistent (Figure 3). All five satellite-derived SOS measures along with latitudinal gradients correlated significantly with each other ( $P < 0.05$ ). In general, the ordinal ranking of SOS measures is HANTS > Midpoint > Logistic > Polyfit  $\approx$  Timesat. For all of these methods, SOS is stable between 36°N and 50°N and gradually becomes earlier at lower and higher latitudes (Figure 3). This pattern obviously varies with ground phenology. The FLD of woody plants delayed linearly with latitude ( $P < 0.05$ , Figure 3). Because the entire 8\*8 km pixels

TABLE 2: Summary of five methods in estimating SOS from satellite data. The number for each method is defined for the purpose of distinguishing the satellite-derived SOS measures from ground phenophases in Table 1.

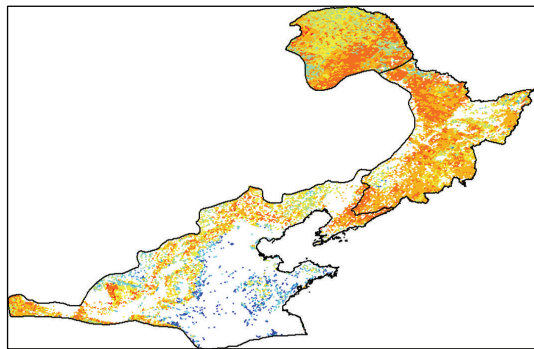
No.	Methods	Curve approaches	SOS determination approaches	Reference
13	Polyfit	Polynomial function	Threshold by the timing of greatest relative change in multi-year averaged series	[17]
14	Logistic	Piecewise logistic functions	Maximum relative change	[24]
15	HANTS	Fourier transformation	Maximum increase	[33]
16	Midpoint	Spline functions	Midpoint	[27]
17	Timesat	Savitzky-Golay filter	20% of NDVI amplitude	[28]



Mean SOS (DOY)



(a)



Maximum difference (days)



(b)

FIGURE 2: (a) The start of season (SOS) averaged from the results of the five methods in the 1982–2006 period and (b) the maximum difference between the five satellite-derived SOS measurements.

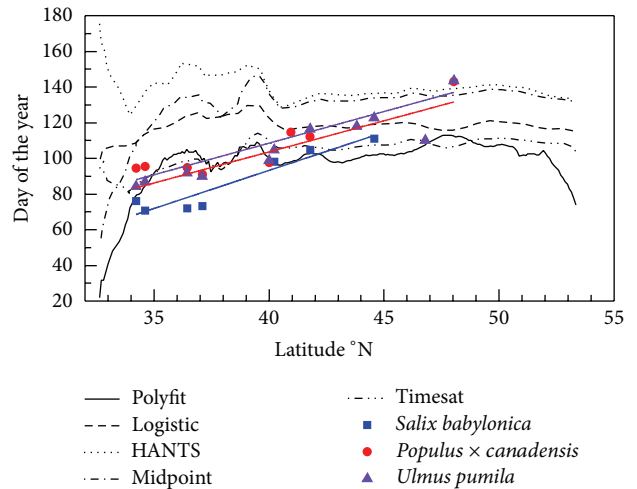
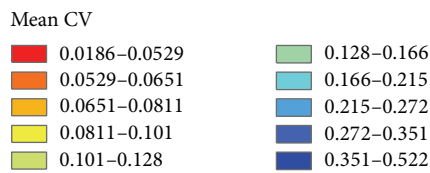
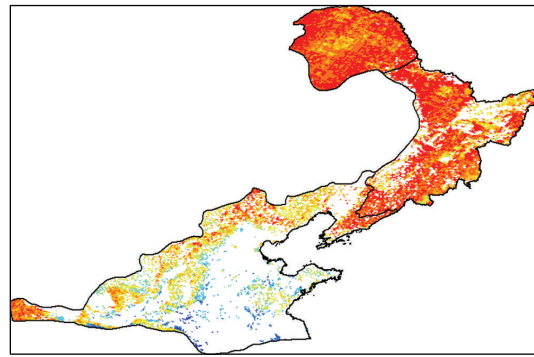


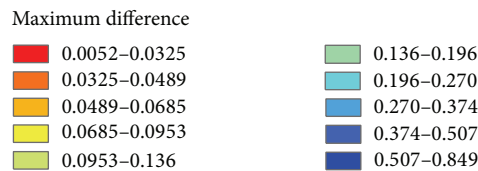
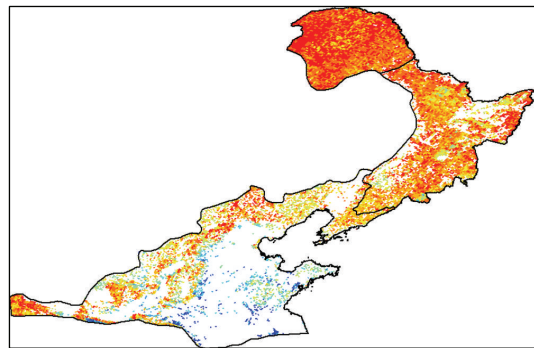
FIGURE 3: The variation of five satellite-derived SOS measures averaged from pixels of broadleaf forest and mean FLD of three broadleaf plants along with latitude. Purple, red, and blue lines are regressions lines for FLD of the three broadleaved plant species, respectively.

along the latitudinal gradient have different plant species compositions, the differences between satellite-derived SOS measures and ground phenology in spatial patterns are expectable.

3.2. Assessment of Temporal Variability of SOS. The variability of SOS obtained through the above five methods is represented by the mean CV of each method. The CV in the northern parts of the study region is relatively smaller, suggesting that the SOS in Northeast China is more stable than that in North China (Figure 4(a)). In regard to vegetation types, the CV of grass-forb reaches up to 0.124, which is the most variable (Table 3). Scrub and steppe both have a CV of 0.088. SOS of the needleleaf forest, mixed forest, broadleaf forest, meadow, swamp, and alpine vegetation is less variable, with their CV ranging from 0.060 to 0.069. Individual SOS methods often differ in CV, especially in North China (Figure 4(b)). Across the study area, the maximum difference between the CV of five satellite-derived SOS measures ranges from 0.019 to 0.523 with a mean of 0.077



(a)



(b)

FIGURE 4: (a) The coefficient of variation (CV) of satellite-derived SOS measures (1982–2006) averaged from the results of the five methods and (b) maximum difference among the CV of five satellite-derived SOS measures.

(Figure 4(b)), suggesting that different SOS methods have different interannual variability.

For the five satellite-derived SOS measures in pixels with broadleaf forest and ground FLD of 12 broadleaf plants, the mean CV (1982–2006) is significantly different (Figure 5, ANOVA,  $P < 0.05$ ). The mean CV of Logistic and Timesat is significantly greater than that of ground phenology (Tukey multiple comparison,  $P < 0.05$ ). The mean CV of HANTS and Polyfit is a little greater than that of ground phenology, but the differences are not statistically significant

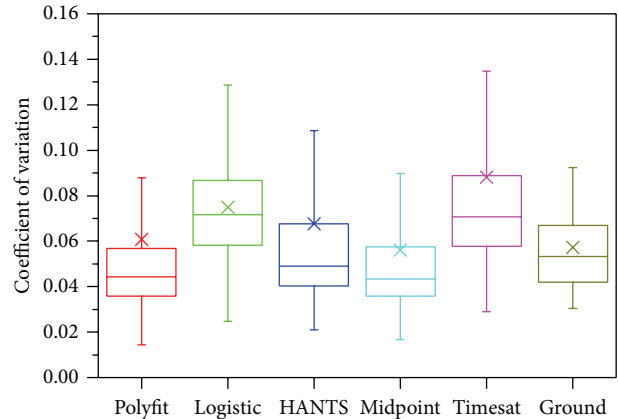


FIGURE 5: Boxplot of the coefficient of variation (CV) for five satellite-derived SOS measures in pixels with broadleaf forest and ground FLD time series at 12 sites. The bottom and top of the box are the 25th and 75th percentile, and the band near the middle of the box is the median. The  $x$  designates the mean value.

(see Figure 5). The mean CV of the Midpoint method (0.056) is closest to the CV of ground phenology (0.057).

**3.3. Correlation between Satellite and Ground-Based Phenology.** The correlation coefficients between time series of five SOS measures and FLD at each CPON site are shown in Figure 6 and summarized in Table 4. The correlations of the five satellite-derived measures are significant in most cases. Especially for the Midpoint method, significant Pearson's correlation coefficients between the Midpoint method and other methods are found at 8 or more sites (Table 4). HANTS method exhibits less consistency with other SOS methods except Midpoint (significant Pearson's correlation coefficients are found at only 1–3 sites).

The time series of plant phenophases observed at the same sites usually correlated significantly with each other (Figure 6). Regarding the relationship between the SOS and ground phenology, at least 14 of 85 cases showed significant correlations (Figure 6, Table 4) and 40 of 85 cases (47.1%) showed significant correlation for the Midpoint method. The numbers of significant correlations for other methods are much less than for the Midpoint method. Only 14, 14, 20, and 23 significant correlations from 85 cases could be detected for Logistic, Timesat, Polyfit, and HANTS methods, respectively. Therefore, SOS measures derived from the Midpoint method show the closest relationship with ground phenology.

In comparison with the 1982–2006 mean dates of ground phenophases, Midpoint, HANTS, Polyfit, and Logistic methods have significant  $R^2$  ( $P < 0.05$ , Figure 7). Timesat had  $R^2$  close to zero. The SOS measures based on the Midpoint method can explain 45% of interannual variability of ground phenophases at maximum although they are about 20 days later than the ground first leaf date.

**3.4. SOS Trends in China's Temperate Monsoon Area.** Through the above analysis, the Midpoint method was more

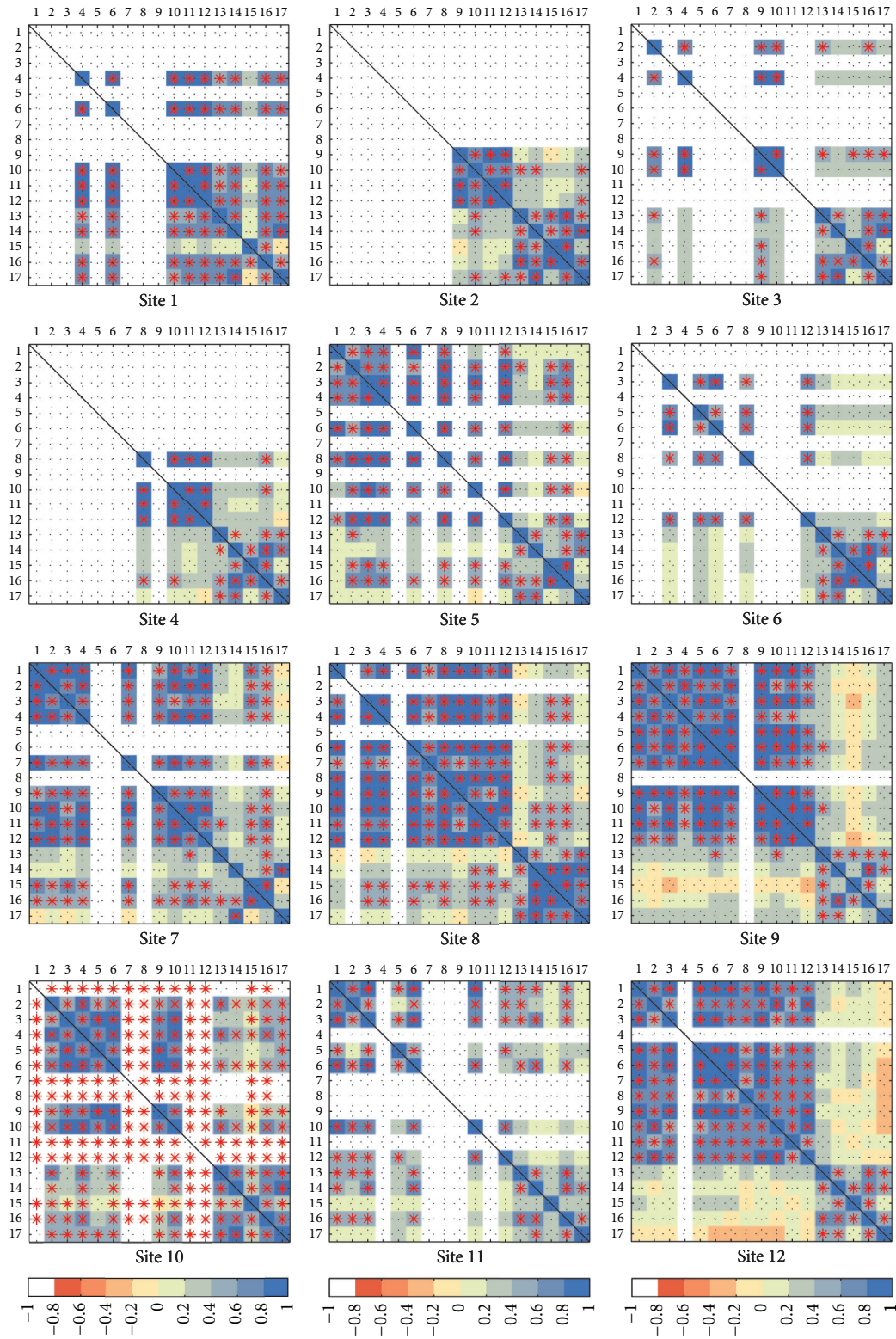


FIGURE 6: Pearson's correlation coefficients between time series of ground phenophases and five satellite-derived SOS measures at each site. The red stars mark the significant correlations ( $P < 0.05$ ). White color indicates no ground observation data. The numbers of ground phenophases (numbers 1–12) correspond to the numbers in Table 1. The numbers of SOS methods (numbers 13–17) correspond to the numbers in Table 2.

TABLE 3: The start of season (SOS) and coefficient of variation (1982–2006) averaged from the results of the five methods for each vegetation type.

Vegetation types	Number of pixels	Mean DOY	Mean SOS	Mean CV
Needleleaf forest	2496	119	4/28	0.069
Mixed forest	263	119	4/27	0.060
Broadleaf forest	4783	119	4/28	0.069
Scrub	1474	121	4/30	0.088
Steppe	401	138	5/16	0.088
Grass-forb	793	123	5/2	0.124
Meadow	1276	125	5/4	0.064
Swamp vegetation	619	124	5/2	0.063
Alpine vegetation	3	125	5/3	0.067

TABLE 4: The proportions of significant Pearson's  $R$  ( $P < 0.05$ ) between time series of ground phenophases and five satellite-derived SOS measures.

Methods	Ground	Polyfit	Logistic	Hants	Midpoint	Timesat
Polyfit	20/85	—	11/12	3/12	12/12	9/12
Logistic	14/85	11/12	—	5/12	12/12	12/12
HANTS	23/85	3/12	5/12	—	11/12	1/12
Midpoint	40/85	12/12	12/12	11/12	—	8/12
Timesat	14/85	9/12	12/12	1/12	8/12	—

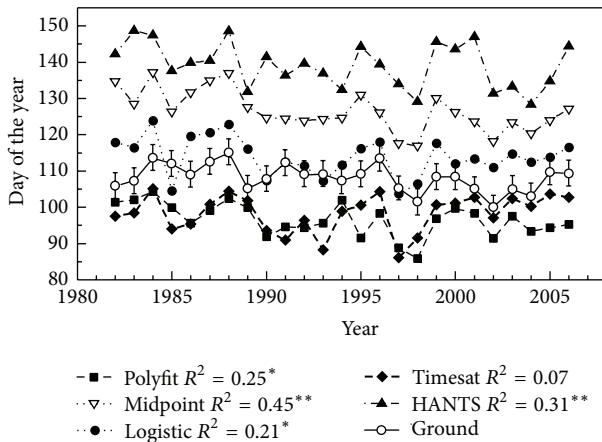


FIGURE 7: Comparison of five satellite-derived SOS measures and ground phenophases averaged over 12 sites from 1982 to 2006. Ground phenophases were first averaged to each site and then for all 12 sites across the region (note that the different sites have different sets of species). The missing ground observation data was interpolated by phenological models described by Ge et al. [8]. The error bar represents the uncertainty due to the interpolated data by models. Variances of ground phenophases explained by each SOS result ( $R^2$ ) are shown. \*  $P < 0.05$ , \*\*  $P < 0.01$ .

closely related to ground observations than other methods, so we investigated the trends of SOS using the Midpoint method. The SOS trends in China's temperate monsoon area from 1982 to 2006 are obvious (Figure 8). For all biomes

(except cultivated vegetation), more than half of the area showed significantly earlier trends ( $P < 0.05$ ). Especially for the needleleaf forest, 57.5% of the distribution area exhibited significantly earlier SOS trends with a mean of  $-0.22$  days  $\text{year}^{-1}$ . The delayed SOS trends ( $P < 0.05$ ) were detected in only 5.3% of the natural vegetation area (Table 5). The swamp had the maximum area proportion of 13.7% towards later SOS, while the needleleaf forest had the minimum area proportion of 1.6% towards later SOS (Table 5). Overall, the linear trends of SOS over the temperate monsoon area of China were  $-0.13$  days  $\text{year}^{-1}$  ( $P = 0.15$ , Figure 9). In addition, the year 1998 can be shown to have been a turning point during which the SOS trends changed (Figure 9). The linear trend in SOS before 1998 was  $-0.39$  days  $\text{year}^{-1}$  ( $P = 0.03$ ), while the SOS showed delaying trends of  $0.45$  days  $\text{year}^{-1}$  from 1998 to 2006 ( $P = 0.31$ ).

#### 4. Discussion

Among the satellite-derived SOS measures using the five most common methods, SOS differed in average day of the year by more than 100 days (Figure 2) and in CV by more than 0.8 (Figure 4) in some pixels. These results were in agreement with other studies [11, 18]. The nearly almost consistent latitudinal patterns (Figure 3) and frequent significant correlations among five satellite-derived SOS measures (Figure 6) suggest, however, that the SOS methods may simply detect different portions of the annual vegetation activity [18]. It is worth

TABLE 5: The percentage of pixels with significant earlier or later SOS trends for each vegetation type.

Vegetation Types	Number of pixels	Earlier SOS		Later SOS		No trends
		%	Trends	%	Trends	%
Needleleaf forest	2496	57.5	-0.18	1.6	0.96	40.9
Mixed forest	263	48.7	-0.11	2.7	0.93	48.6
Broadleaf forest	4783	49.1	-0.18	6.1	0.93	44.8
Scrub	1474	49.2	-0.33	2.6	0.96	48.2
Steppe	401	47.1	-0.30	3.7	1.13	49.2
Grass-forb	793	44.5	-0.53	2.3	1.51	53.2
Meadow	1276	49.0	-0.20	11.2	1.04	39.8
Swamp vegetation	619	54.6	-0.15	14.1	1.11	31.3
Alpine vegetation	3	33.3	-0.62	0.0	—	66.7
Total	12108	50.7	-0.22	5.3	1.00	44.0

Unit of trends: days year<sup>-1</sup>.

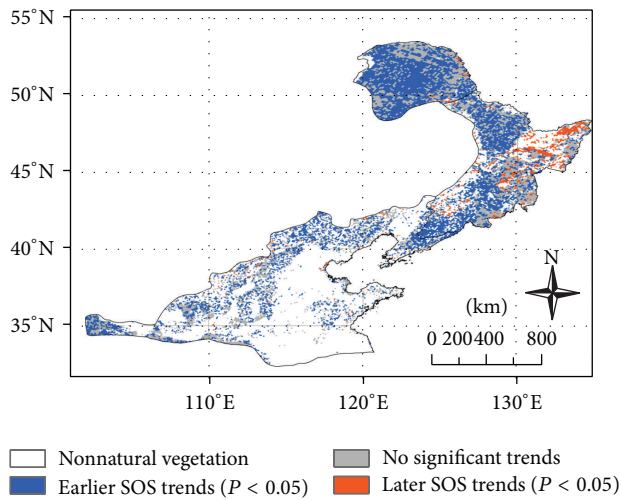


FIGURE 8: Location of trends in SOS (1982–2006) calculated using the Midpoint method. The pixels with earlier SOS trends ( $P < 0.05$ ), no significant trends ( $P > 0.05$ ), and later SOS trends ( $P < 0.05$ ) occupy 50.7%, 44.0%, and 5.3% of the total natural vegetation area, respectively.

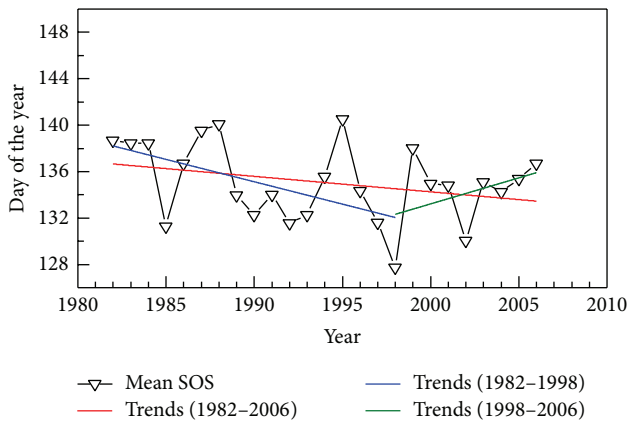


FIGURE 9: The annual SOS in China's temperate monsoon area based on the Midpoint method. Regression for the periods 1982–2006, 1982–1998, and 1998–2006 is shown.

noting that these results were based on a given satellite-based NDVI dataset with identical data sources, durations, compositing schemes, and spatial resolutions. If the data sources were different, the significant correlations between the various satellite-derived SOS measures would be less frequent [11].

Changing temperatures influence the variability of specific plant phenophases observed on the ground as well as spatially integrated SOS as seen from space [35]. Therefore, theoretically, the time series of the ground phenophases and satellite-derived SOS would highly correspond in their inter-annual variability. In this study, however, only 16.5–45.4% of the cases showed significant correlations between time series of FLD and satellite-derived SOS measures. The infrequent correlations can be attributed to the contrasting properties of satellite datasets and ground observation data. Satellite vegetation index datasets typically have coarse temporal resolutions (10–15 days) and spatial resolutions (0.25–8 km), while ground data generally consist of point values. This is the so-called point versus pixel problem [18]. Because the ground data in this study lacked detailed sampling schemes, there is a high probability that the species investigated cannot represent the overall phenological developments in an entire 8 km pixel. In addition, the different sites have different sets of species, which may be a source of variation in the comparison to satellite data. Although these uncertainties exist, the Midpoint method tracked the ground phenophases with high  $R^2$  (45%), suggesting that the interannual variability of satellite-derived SOS measures and spring phenophases of ground observed species is comparable even in a pixel with high land cover heterogeneity.

The time series of mean FLD for the 12 species investigated in this study advanced at a rate of 0.22 days year<sup>-1</sup> from 1982 to 2006 ( $P < 0.05$ , Figure 7). This result agrees with earlier spring phenological trends found in previous studies. For instance, 22 woody plants flowered earlier in eastern China during 1963–2006 period [36]. The modeled first leaf date of *Fraxinus chinensis* advanced at a rate of 0.11 days year<sup>-1</sup> from 1952 to 2007 [37]. Compared with ground observations, satellite data can provide comprehensive coverage even though they can only reach back for three decades.

The trends in satellite-derived SOS measures match ground observations. We found a remarkable earlier SOS trend in 50.7% of the natural vegetation area with a mean of 0.22 days year<sup>-1</sup> (Figure 8). When the contributions of pixels with insignificant or later trends were considered, the overall trend in SOS across the study area was only 0.13 days year<sup>-1</sup> ( $P = 0.15$ ). As indicated by a previous study [38], these changes in SOS are mostly driven by climate change, especially by temperature rise.

Our results highlight that ground observations have a certain linkage with remote sensing data, but approaches using limited numbers of plants face considerable challenges. Integrating and comparing ground phenology and satellite-derived SOS measures need more detailed field observation, such as investigating the land cover of each pixel, the proportions of individual species in a community, and the rate of phenological status (rather than just recording the date of discrete events). For example, Liang et al. [39] employed intensive field observation to address the problem of the significant spatiotemporal scale mismatch between satellite-measured land surface phenology and ground phenology. They found that the MODIS/EVI-derived SOS measure was able to predict landscape phenology of full bud burst date accurately [39]. To make detailed ground-based observations, however, requires much more labor. Recently, “near surface” remote sensing using digital photography has become commonplace [40]. Automated digital cameras, as inexpensive, easy-to-use multispectral sensors, can improve both spatial and temporal resolution with less labor [41]. Therefore, digital repeat photography has great potential for determining the relationships between the various measures of vegetation development in the future.

## 5. Conclusions

In this study, we assessed five SOS methods based on the ground FLD data of 12 deciduous broadleaf trees at 12 sites of CPON. The satellite-derived SOS measures varied greatly among the five methods. Furthermore, the variability of each of the five satellite-derived SOS measures was significantly different from each other. Through the correlation analysis between time series of five satellite-derived SOS measures and ground phenology, we found that the Midpoint method was most consistent with ground observations. Based on the Midpoint method, therefore, significantly earlier trends in SOS from 1982 to 2006 have been detected in 50.7% of the natural vegetation in the study area.

## Conflict of Interests

The authors declare that there is no conflict of interests regarding the publication of this paper.

## Acknowledgments

This research was supported by Key Project of National Natural Science Foundation of China (NSFC, no. 41030101), National Basic Research Program of China (2012CB955304),

NSFC project (no. 41171043), and “Strategic Priority Research Program-Climatic Change: Carbon Budget and Relevant Issues” of the Chinese Academy of Sciences (no. XDA05090301).

## References

- [1] M. D. Schwartz, *Phenology: An Integrative Environmental Science*, Kluwer Academic Publishers, Dordrecht, The Netherlands, 2003.
- [2] G.-R. Walther, E. Post, P. Convey et al., “Ecological responses to recent climate change,” *Nature*, vol. 416, no. 6879, pp. 389–395, 2002.
- [3] C. Rosenzweig, G. Casassa, D. J. Karoly et al., “Assessment of observed changes and responses in natural and managed systems,” in *Climate Change 2007: Impacts, Adaptation and Vulnerability. Contribution of Working Group II to the Fourth Assessment Report of the Intergovernmental Panel on Climate Change*, M. L. Parry, O. F. Canziani, J. P. Palutikof, P. J. van der Linden, and C. E. Hanson, Eds., pp. 79–131, Cambridge University Press, Cambridge, UK, 2007.
- [4] E. E. Cleland, I. Chuine, A. Menzel, H. A. Mooney, and M. D. Schwartz, “Shifting plant phenology in response to global change,” *Trends in Ecology and Evolution*, vol. 22, no. 7, pp. 357–365, 2007.
- [5] R. Stckli, T. Rutishauser, I. Baker, M. A. Liniger, and A. S. Denning, “A global reanalysis of vegetation phenology,” *Journal of Geophysical Research G: Biogeosciences*, vol. 116, no. 3, 2011.
- [6] F. W. Badeck, A. Bondeau, K. Böttcher et al., “Responses of spring phenology to climate change,” *New Phytologist*, vol. 162, no. 2, pp. 295–309, 2004.
- [7] T. H. Sparks and A. Menzel, “Observed changes in seasons: an overview,” *International Journal of Climatology*, vol. 22, no. 14, pp. 1715–1725, 2002.
- [8] Q. Ge, H. Wang, and J. Dai, “Shifts in spring phenophases, frost events and frost risk for woody plants in temperate China,” *Climate Research*, vol. 57, no. 3, 2013.
- [9] J. T. Morissette, A. D. Richardson, A. K. Knapp et al., “Tracking the rhythm of the seasons in the face of global change: phenological research in the 21st century,” *Frontiers in Ecology and the Environment*, vol. 7, no. 5, pp. 253–260, 2008.
- [10] A. Barr, T. A. Black, and H. McCaughey, “Climatic and phenological controls of the carbon and energy balances of three contrasting boreal forest ecosystems in western Canada,” in *Phenology of Ecosystem Processes*, A. Noormets, Ed., pp. 3–34, Springer, New York, NY, USA, 2009.
- [11] M. D. Schwartz and J. M. Hanes, “Intercomparing multiple measures of the onset of spring in eastern North America,” *International Journal of Climatology*, vol. 30, no. 11, pp. 1614–1626, 2010.
- [12] S. Piao, P. Friedlingstein, P. Ciais, N. Viovy, and J. Demarty, “Growing season extension and its impact on terrestrial carbon cycle in the Northern Hemisphere over the past 2 decades,” *Global Biogeochemical Cycles*, vol. 21, no. 3, p. B3018, 2007.
- [13] M. D. Schwartz and B. C. Reed, “Surface phenology and satellite sensor-derived onset of greenness: an initial comparison,” *International Journal of Remote Sensing*, vol. 20, no. 17, pp. 3451–3457, 1999.
- [14] M. D. Schwartz, B. C. Reed, and M. A. White, “Assessing satellite-derived start-of-season measures in the conterminous USA,” *International Journal of Climatology*, vol. 22, no. 14, pp. 1793–1805, 2002.

- [15] N. Cong, S. Piao, A. Chen et al., "Spring vegetation green-up date in China inferred from SPOT NDVI data: a multiple model analysis," *Agricultural and Forest Meteorology*, vol. 165, pp. 104–113, 2012.
- [16] T. Ma and C. Zhou, "Climate-associated changes in spring plant phenology in China," *International Journal of Biometeorology*, vol. 56, no. 2, pp. 269–275, 2012.
- [17] S. Piao, J. Fang, L. Zhou, P. Ciais, and B. Zhu, "Variations in satellite-derived phenology in China's temperate vegetation," *Global Change Biology*, vol. 12, no. 4, pp. 672–685, 2006.
- [18] M. A. White, K. M. de Beurs, K. Didan et al., "Intercomparison, interpretation, and assessment of spring phenology in North America estimated from remote sensing for 1982–2006," *Global Change Biology*, vol. 15, no. 10, pp. 2335–2359, 2009.
- [19] S. Studer, R. Stöckli, C. Appenzeller, and P. L. Vidale, "A comparative study of satellite and ground-based phenology," *International Journal of Biometeorology*, vol. 51, no. 5, pp. 405–414, 2007.
- [20] Editorial Board of the Vegetation Map of China, *Vegetation Map of the People's Republic of China (1:10000000)*, Geological Publishing House, Beijing, China, 2007.
- [21] M. W. Wan and X. Z. Liu, *China's National Phenological observational Criterion*, Science Press, Beijing, China, 1979.
- [22] C. J. Tucker, J. E. Pinzon, M. E. Brown et al., "An extended AVHRR 8-km NDVI dataset compatible with MODIS and SPOT vegetation NDVI data," *International Journal of Remote Sensing*, vol. 26, no. 20, pp. 4485–4498, 2005.
- [23] L. Zhou, R. K. Kaufmann, Y. Tian, R. B. Myneni, and C. J. Tucker, "Relation between interannual variations in satellite measures of northern forest greenness and climate between 1982 and 1999," *Journal of Geophysical Research D: Atmospheres*, vol. 108, no. 1, p. 4004, 2003.
- [24] X. Zhang, M. A. Friedl, C. B. Schaaf et al., "Monitoring vegetation phenology using MODIS," *Remote Sensing of Environment*, vol. 84, no. 3, pp. 471–475, 2003.
- [25] G. J. Roerink, M. Menenti, and W. Verhoef, "Reconstructing cloudfree NDVI composites using Fourier analysis of time series," *International Journal of Remote Sensing*, vol. 21, no. 9, pp. 1911–1917, 2000.
- [26] M. A. White, P. E. Thornton, and S. W. Running, "A continental phenology model for monitoring vegetation responses to interannual climatic variability," *Global Biogeochemical Cycles*, vol. 11, no. 2, pp. 217–234, 1997.
- [27] M. A. White, R. R. Nemani, P. E. Thornton, and S. W. Running, "Satellite evidence of phenological differences between urbanized and rural areas of the eastern United States deciduous broadleaf forest," *Ecosystems*, vol. 5, no. 3, pp. 260–273, 2002.
- [28] P. Jönsson and L. Eklundh, "Seasonality extraction by function fitting to time-series of satellite sensor data," *IEEE Transactions on Geoscience and Remote Sensing*, vol. 40, no. 8, pp. 1824–1832, 2002.
- [29] J. Chen, P. Jönsson, M. Tamura, Z. Gu, B. Matsushita, and L. Eklundh, "A simple method for reconstructing a high-quality NDVI time-series data set based on the Savitzky-Golay filter," *Remote Sensing of Environment*, vol. 91, no. 3–4, pp. 332–344, 2004.
- [30] R. Lee, F. Yu, K. P. Price, J. Ellis, and P. Shi, "Evaluating vegetation phenological patterns in Inner Mongolia using NDVI time-series analysis," *International Journal of Remote Sensing*, vol. 23, no. 12, pp. 2505–2512, 2002.
- [31] W. J. D. van Leeuwen, "Monitoring the effects of forest restoration treatments on post-fire vegetation recovery with MODIS multitemporal data," *Sensors*, vol. 8, no. 3, pp. 2017–2042, 2008.
- [32] J. I. Fisher, J. F. Mustard, and M. A. Vadeboncoeur, "Green leaf phenology at Landsat resolution: scaling from the field to the satellite," *Remote Sensing of Environment*, vol. 100, no. 2, pp. 265–279, 2006.
- [33] G. J. Roerink, M. Menenti, W. Soepboer, and Z. Su, "Assessment of climate impact on vegetation dynamics by using remote sensing," *Physics and Chemistry of the Earth*, vol. 28, no. 1–3, pp. 103–109, 2003.
- [34] The R Core Team, *R: A Language and Environment for Statistical Computing*, R Foundation for Statistical Computing, Vienna, Austria, 2014.
- [35] T. Rutishauser, J. Luterbacher, F. Jeanneret, C. Pfister, and H. Wanner, "A phenology-based reconstruction of interannual changes in past spring seasons," *Journal of Geophysical Research G: Biogeosciences*, vol. 112, no. 4, p. 4016, 2007.
- [36] Q. Ge, J. Dai, J. Zheng et al., "Advances in first bloom dates and increased occurrences of yearly second blooms in eastern China since the 1960s: further phenological evidence of climate warming," *Ecological Research*, vol. 26, no. 4, pp. 713–723, 2011.
- [37] H. Wang, J. Dai, and Q. Ge, "The spatiotemporal characteristics of spring phenophase changes of *Fraxinus chinensis* in China from 1952 to 2007," *Science China Earth Sciences*, vol. 55, no. 6, pp. 991–1000, 2012.
- [38] N. Cong, T. Wang, H. Nan et al., "Changes in satellite-derived spring vegetation green-up date and its linkage to climate in China from 1982 to 2010: a multimethod analysis," *Global Change Biology*, vol. 19, no. 3, pp. 881–891, 2013.
- [39] L. Liang, M. D. Schwartz, and S. Fei, "Validating satellite phenology through intensive ground observation and landscape scaling in a mixed seasonal forest," *Remote Sensing of Environment*, vol. 115, no. 1, pp. 143–157, 2011.
- [40] A. D. Richardson, J. P. Jenkins, B. H. Braswell, D. Y. Hollinger, S. V. Ollinger, and M.-L. Smith, "Use of digital webcam images to track spring green-up in a deciduous broadleaf forest," *Oecologia*, vol. 152, no. 2, pp. 323–334, 2007.
- [41] R. Ide and H. Oguma, "Use of digital cameras for phenological observations," *Ecological Informatics*, vol. 5, no. 5, pp. 339–347, 2010.



# Hindawi

Submit your manuscripts at  
<http://www.hindawi.com>

